International Journal of Applied Engineering Research ISSN 0973-4562 Volume 10, Number 19 (2015) pp 40010-40020

Modified Dugdale Model for Three Equal Collinear Straight Cracks: A Theoretical Analysis

Naved Akhtar

Department of Mathematics, Jamia Millia Islamia (Central University), New Delhi-110 025, India naved.a86@gmail.com

S. Hasan

Department of Mathematics, Jamia Millia Islamia (Central University), New Delhi-110 025, India drshehzadhasan@gmail.com

Abstract
In this paper, Dugdale-Barenblatt model has been modified to evaluate load bearing capacity of an infinite isotropic elastic-perfectly plastic plate damage by three straight collinear quasi-static cracks. These cracks open in mode-I type deformation when infinite boundary of the plate is subjected to uniform tensile stresses acting perpendicular to the faces of cracks. As a result, yield zones develop at each crack tip. Sometimes, structure fails at stress which is well below the yield stress of the material. Therefore, yield zones are assume to be subjected by a quadratically varying yield stress distribution applied perpendicular to the faces of the yield zones to stop further opening of cracks. The problem is solved using complex variable method and analytical expressions are derived for stress intensity factors(SIF), crack tip-opening displacement (CTOD) under small scale yielding. Numerical results are obtained for yield zone length and crack tip-opening displacement at each crack tip and reported graphically. These numerical results are compared with the results of two equal collinear straight cracks and/or a single straight crack under same mechanical loading conditions.

Key words Stress intensity factor, crack-tip-opening displacement, Dugdale model, multiple cracks.

2010 Mathematics Subject Classification74R05, 74R10

1. Introduction

Failure of engineering material due to cracks or crack like defects is a serious problem. Strength of the material reduces in the presence of such defects [1]. Therefore, to know the residual strength of the materials in the presence of cracks and modelling such a situation is important for the safety and durability of the structures. Dugdale model[2] was used widely to evaluate residual strength of the material containing crack(s). In most of the cases yield stress of the plate is assume to be constant, but in few cases yield stress of the plate be considered as linearly and quadratically varying. Kanninen[3] modified the model for linearly varying stress distribution, while Harrop[4] used Dugdale hypothesis to determine crack tip opening displacement when plastic zones are subjected to parabolic stress distribution. Theocaris et al.[5] used Dugdale model to evaluate load-bearing capacity of three different types of strain hardening materials and mechanical loading conditions. Dual scale crack model was discussed in [6], [7] for macro and microscopic cracks under linearly varying stress distribution.

Dugdale model was not limited to just a single crack, but also used to solve multiple crack problems for variety of materials, different crack configurations and various mechanical loading conditions. Theocaris[8] used Dugdale model to determine the size of plastic zone at each crack tip of two collinear unequal straight cracks and also discuss the case of plastic zone coalescence at the internal tips of two cracks. A strip yield model for two equal straight cracks was also discussed by Collins et al.[9] to determine the length of yield zones and for three equal straight cracks by Hasan et al.[10]. On increasing stresses applied at the boundary of the plate yield zones between closely, located cracks were coalesced. Feng et al.[11] discussed the case of coalescence of plastic zones between two collinear straight cracks in a quasi-brittle material under plane stress distribution. Bhargava et al.[12] used Dugdale model to study the load bearing capacity of an infinite plate weakened by two straight collinear unequal asymmetrically situated cracks under quadratically varying stress distribution.

Although now it is easy to find out closed form solution for a single Dugdale crack. But, still it is mathematically difficult to solve multiple crack problems. Various approaches have been used to simplify mathematical complexities for solving multiple crack problems. Complex variable method was used to determine crack-tip-opening displacement for two asymmetrically situated cracks with coalesced yield zones in [13], for four symmetrically situated cracks with coalesced interior yield zones in[14], for finite and semi infinite cracks [15], Weight function approach was used by Wu and Xu[16] and there are so many examples.

The paper deals with a mathematically complex problem of three collinear straight cracks weaken an infinite elastic perfectly plastic plate. Cracks open in mode-I type deformation and yield zones develop at each crack tip due to stresses applied at the infinite boundary of the plate. It is observed by Gdoutos[17] that some of the structure fails at a stress which is well below the yield stress of the material, therefore the developed yield zones are assumed to be subjected to a quadratically varying stress distribution to arrest further opening of cracks. Closed form solution of the problem is obtained using complex variable method. Analytical expressions are obtained for SIF, components of displacement and CTOD at each crack tip. Numerical results are obtained and analyzed for yield zone length, load required ratio and CTOD at each cracks tip.

Nomenclature

$D_i (i = 0,1,2,3)$	constants of the problem.
E	Young's modulus.
$F(\theta,k)$, $E(\theta,k)$, $\Pi(\theta,\alpha^2,k)$	incomplete elliptic integral of first, second and third kind respectively.
$L_i (i = 1,2,3)$	length of original cracks.
$P_n(z)$	polynomial of degree *n*.
$\delta(x)$	crack tip-opening displacement at the crack tip *x*.
$\pm a_1, \pm b_1, \pm c_1$	original crack tips.
$\pm a, \pm b, \pm c$	extended crack tips.
$p(t), q(t)$	applied stresses on the yield zones.
u, v	components of displacement.
$z = x + iy$	complex variable.
Γ'	$-\frac{1}{2}(N_1 - N_2)e^{-2i\alpha}, N_1$ and N_2 are the values of principal stresses at infinity, α be the angle between N_1 and the *ox*-axis
$\Gamma_i (i = 1,2,\ldots,6)$	length of yield zones.
$\Omega(z) = \omega'(z)$, $\Phi(z) = \phi'(z)$	complex potential functions.
γ	Poisson's ratio.
μ	shear modulus.
κ	$= \frac{3-\gamma}{1+\gamma}$ for the plane-stress, $= 3 - 4\gamma$ for the plane-strain.
X_x, Y_y, X_y	components of stress.
σ_∞	remotely applied stress at theinfinite boundary of the plate.
σ_{ye}	yield stress of the plate.

2. Mathematical formulation

In two dimensional theory of elasticity, components of stresses X_x, Y_y, X_y and displacements (u, v) may be expressed in terms of two complex potential functions $\Phi(z), \Omega(z)$ as given by Muskhelishvili[18]

$$X_x + Y_y = 2[\Phi(z) + \overline{\Phi(z)}], \tag{1}$$

$$Y_y - iX_y = \Phi(z) + \Omega(\bar{z}) + (z - \bar{z})\overline{\Phi'(z)}, \tag{2}$$

$$2\mu(u + iv) = \kappa\phi(z) - \omega(\bar{z}) - (z - \bar{z})\overline{\Phi(z)}. \tag{3}$$

where line over a function or a variable denotes its complex conjugate and prime over the function denotes differentiation. Consider an infinite isotropic elastic-perfectly plastic plate occupy *xy*-plane containing *n* straight cuts L_i (*i=1,2,3,…,n*) lying along real axis. Let $X_y^\pm, Y_y^\pm$ be the stress distributions acting on the rims of the cracks, where superscript $+$, $-$ denote the upper and lower rim of the cracks. Eqs.1 and 2 may be expressed in terms of two problems of linear relationships under the assumption $\lim_{y \to 0} y\Phi'(t + iy) = 0$,

$$\Phi^+(t) + \Omega^-(t) = Y_y^+ - iX_y^+, \tag{4}$$

$$\Phi^-(t) + \Omega^+(t) = Y_y^- - iX_y^-, \tag{5}$$

on *L*, where $L = \bigcup_{i=1}^{n} L_i$.

Closed form solution of the problems expressed in Eqs.4 and 5 may be obtained using a detailed methodology given in [18] as:

$$\Phi(z) = \Phi_0(z) + \frac{P_n(z)}{X(z)} - \frac{1}{2}\overline{\Gamma}', \tag{6}$$

$$\Omega(z) = \Omega_0(z) + \frac{P_n(z)}{X(z)} + \frac{1}{2}\overline{\Gamma}'. \tag{7}$$

where

$$\Phi_0(z) = \frac{1}{2\pi i X(z)} \int_{\bigcup_{i=1}^{n} L_i} \frac{X^+(t)p(t)}{t - z} dt + \frac{1}{2\pi i} \int_{\bigcup_{i=1}^{n} L_i} \frac{q(t)}{t - z} dt, \tag{8}$$

$$\Omega_0(z) = \frac{1}{2\pi i X(z)} \int_{\bigcup_{i=1}^{n} L_i} \frac{X^+(t)p(t)}{t - z} dt - \frac{1}{2\pi i} \int_{\bigcup_{i=1}^{n} L_i} \frac{q(t)}{t - z} dt, \tag{9}$$

$$p(t) = \frac{1}{2}[Y_y^+ + Y_y^-] - \frac{i}{2}[X_y^+ + X_y^-]$$

$$, q(t) = \frac{1}{2}[Y_y^+ - Y_y^-] - \frac{i}{2}[X_y^+ - X_y^-], \tag{10}$$

$$X(z) = \prod_{k=1}^{n} \sqrt{z - a_k}\sqrt{z - b_k},$$

$$P_n(z) = D_0 z^n + D_1 z^{n-1} + \ldots + D_n. \tag{11}$$

Constants $D_i (i = 0,1,2,.., n)$ shown in Eq.11 are evaluated using loading condition at an infinite boundary of the plate and single-valuedness condition of displacement around the rims of the cracks or cuts,

$$2(\kappa + 1)\int_{L_i} \frac{P_n(t)}{X(t)} dt + \kappa \int_{L_i} [\Phi_0^+(t) - \Phi_0^+(t)] dt + \int_{L_i} [\Omega_0^+(t) - \Omega_0^-(t)] dt = 0. \tag{12}$$

The mathematical formulation given above is taken from Muskhelishvili[18] for making the paper self-sufficient.

3.Problem description

Consider a multi-site damage (MSD) problem of three equal collinear straight cracks damage an infinite isotropic elastic-perfectly plastic plate. The plate occupies the entire *xy*-plane. The cracks are exist in the plate symmetrically along the real axis, denoted by L_1, L_2, L_3 and occupy the intervals $[-a_1, -b_1]$, $[-c_1, c_1]$, $[b_1, a_1]$ respectively.

International Journal of Applied Engineering Research ISSN 0973-4562 Volume 10, Number 19 (2015) pp 40010-40020

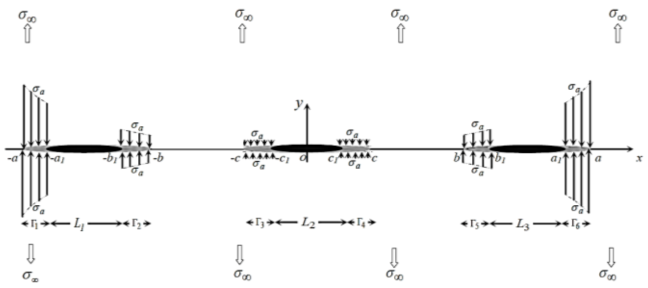

Figure 1: Modified Dugdale model of three equal straight cracks

Infinite boundary of the plate is subjected to a uniform stress distribution $Y_y = \sigma_\infty$. As a result, cracks are open in mode-I (opening mode) type of deformation and yield zones developed at each crack tip. These yield zones are denoted by $\Gamma_i (i = 1,2,3...6)$ and occupy the intervals $(-a,-a_1],[-b_1,-b)$, $(-c,-c_1],[c_1,c),(b,b_1],[a_1,a)$ respectively on ox-axis. It is mention in [17] that some of the structures fail at a stress, which is well below the yield stress of the plate. Therefore, a parabolic stress distribution $Y_y = \frac{t^2}{a^2}\sigma_{ye}$, which is below the yield stress of the plate (say, σ_a), is applied on the rims of the yield zones to stop further opening of cracks, where t is any point of the rims of the yield zones and σ_{ye} is the yield stress of the plate. Entire configuration of the problem is depicted in Fig.1.

4.Solution of the problem

Solution of the main problem defined in Section-3 is obtained by decomposing it into two sub-problems namely problem-A (tensile case, $Y_y = \sigma_\infty$) and problem-B (yield case, $Y_y = \frac{t^2}{a^2}\sigma_{ye}$). These two sub-problems are solved using methodology given in Section-2. Furthermore, the solution of main problem is then obtained on superposing the solutions of two sub-problems.

4.1 Sub-problem A: Tensile stress case

4.1.1 Problem and its solution

Development of yield zones at each crack tip due to remotely applied stresses at the infinite boundary of the plate has been discussed in this section. Consider a loaded infinite isotropic elastic perfectly plastic plate containing three equal collinear cracks. Normal tensile stresses, $Y_y = \sigma_\infty$, act at the infinite boundary of the plate, causes the opening of cracks in mode-I type deformation. Thus, yield zones are developed at each crack tip. The cracks with corresponding yield zones are denoted by $R_1(-a,-b)$, $R_2(-c,c)$ and $R_3(b,a)$. The complete geometrical configuration of the opening case is given in Fig.2.

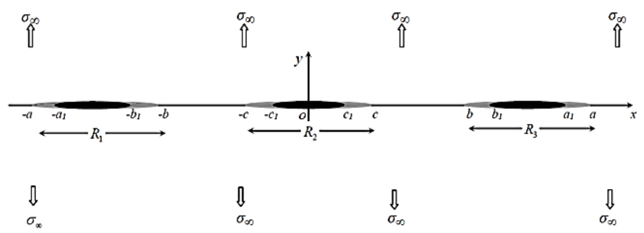

Figure 2: Configuration of the sub-problem-A

Following are the boundary conditions for the opening case

$$Y_y = \sigma_\infty, X_y = 0, when \quad y \to \pm\infty, -\infty < x < \infty, \tag{13}$$

$$Y_y = X_y = 0, when \quad y = 0, x \in \bigcup_{i=1}^{3} L_i, \tag{14}$$

Desired complex potential function $\Phi_A(z)$ may be obtained using methodology given in Section-2 and boundary conditions given Eqs.13 and 14. Hence, for the *sub-problem-A*

$$\Phi_A(z) = \frac{\sigma_\infty}{2}[\frac{1}{X(z)}\{z^3 - z(c^2 + (a^2 - c^2)\lambda^2)\} - \frac{1}{2}], \tag{15}$$

where $\lambda^2 = \frac{E(k)}{F(k)}, k^2 = \frac{a^2 - b^2}{a^2 - c^2}$ and $F(k), E(k)$ are complete elliptical integrals of first and second kind respectively as defined in [19].

4.1.2 Stress intensity factor

Closed form solution for opening mode stress intensity factor at the crack tip $z = t$ may be obtained using the formulae given in [9]

$$K_I = 2\sqrt{2\pi} \lim_{z \to t} \sqrt{z - t}\,\Phi(z). \tag{16}$$

Therefore, analytical expressions for stress intensity factor at each exterior crack tip *a*, *b* and *c* may be written using Eqs. 15 and 16 as,

$$(K_I^A)_a = (\frac{1 - \lambda^2}{k})\sigma_\infty \sqrt{\pi a}, \tag{17}$$

$$(K_I^A)_b = (\frac{\lambda^2 + k^2 - 1}{k\sqrt{1 - k^2}})\sigma_\infty \sqrt{\pi b}, \tag{18}$$

$$(K_I^A)_c = (\frac{\lambda^2}{\sqrt{1 - k^2}})\sigma_\infty \sqrt{\pi c}. \tag{19}$$

Stress intensity factors at each crack tip given in Eqs.17 - 19 are same as given by Tada[20].

4.1.3 Components of displacement

Analytical expressions for the displacement components $v_\infty^\pm(x)$ at cracks tips $\pm a, \pm b$ and $\pm c$ due to stresses, $Y_y = \sigma_\infty$, (acting at the infinite boundary of the plate) may be obtained using Eqs. 3 and 15 . Closed form expressions for $v_\infty^\pm(x)$ may be written as,

$$v_\infty^\pm(\pm a_1) = \pm\frac{2\sigma_\infty}{E}\sqrt{a^2 - c^2}[E(\phi_1(a_1), k) - \lambda^2 F(\phi_1(a_1), k)], \tag{20}$$

International Journal of Applied Engineering Research ISSN 0973-4562 Volume 10, Number 19 (2015) pp 40010-40020
© Research India Publications. http://www.ripublication.com

$$v_\infty^{\pm}(\pm b_1) = \mp\frac{2\sigma_\infty}{E}\sqrt{a^2-c^2}[E(\phi_2(b_1),k)$$
$$-\lambda^2 F(\phi_2(b_1),k) - \frac{k^2 \sin\phi_2(b_1)\cos\phi_2(b_1)}{\sqrt{1-k^2 \sin^2\phi_2(b_1)}}], \tag{21}$$

$$v_\infty^{\pm}(\pm c_1) = \mp\frac{2\sigma_\infty}{E}\sqrt{a^2-c^2}[E(\phi_3(c_1),k)$$
$$-\lambda^2 F(\phi_3(c_1),k) - \tan\phi_3(c_1)\sqrt{1-k^2 \sin^2\phi_3(c_1)}]. \tag{22}$$

4.2 Sub-Problem B: Yield stress case

4.2.1 Problem and its solution

Consider the case, when three collinear straight cracks with yield zones (developed due to applied stresses at the infinite boundary of the plate, as discussed in Section-4.1) exist in an infinite elastic perfectly plastic plate. It is mention in [17] that some of the structures fail at a stress, which is well below the yield stress of the material. Therefore, a quadratically varying yield stress distribution $Y_y = \frac{t^2}{a^2}\sigma_{ye}$, which is below the yield stress of the plate, is applied on the rims of the yield zones in order to seize the growth of cracks. The entire configuration of the sub-problem B is given in Fig.3.

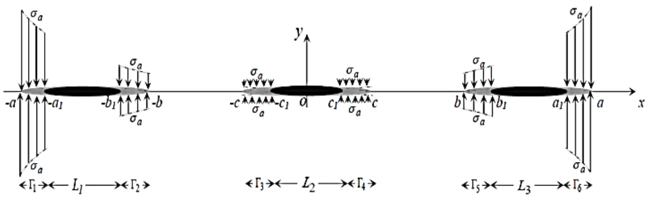

Figure 3: Configuration of the sub-problem-B

The problem is solved under the following boundary conditions

$$Y_y = 0, \quad X_y = 0, when \quad y \to \pm\infty, -\infty < x < \infty. \tag{23}$$

$$Y_y = \frac{t^2}{a^2}\sigma_{ye}, \quad X_y = 0, when \quad y \to 0, x \in \bigcup_{n=1}^{6}\Gamma_n. \tag{24}$$

Using the boundary conditions given in Eqs. 23 and 24 and methodology shown in Section-2, desired complex potential function $\Phi_B(z)$ for the *sub-problem B* may be written as,

$$\Phi_B(z) = \frac{\sigma_{ye}}{2\pi i a^2 X(z)}[\int_{L'}\frac{t^2 X(t)}{t-z}dt$$
$$+ ia^2(D_1 z^2 + D_2 z + D_3)], \tag{25}$$

Where

$$L' = (-a,-a_1] \cup [-b_1,-b) \cup (-c,-c_1]$$
$$\cup [c_1,c) \cup (b,b_1] \cup [a_1,a).$$

In order to derive analytical expression for $\Phi_B(z)$, the integral shown on the right-hand side of the Eq.25 must be evaluated using following relations,

when $\; -a < -b < -c < c < b < t < a,$

$$X(t) = X(-t) = i\sqrt{a^2-t^2}\sqrt{t^2-b^2}\sqrt{t^2-c^2},$$

and

when $\; -a < -b < -c < t < c < b < a$

$$X(t) = X(-t) = -i\sqrt{a^2-t^2}\sqrt{b^2-t^2}\sqrt{c^2-t^2}.$$

Hence, the integral

$$\int_{L'}\frac{t^2 X(t)}{t-z}dt = 2z[\int_{a_1}^{a}\frac{t^2 X(t)}{t^2-z^2}dt + \int_{b}^{b_1}\frac{t^2 X(t)}{t^2-z^2}dt + \int_{c_1}^{c}\frac{t^2 X(t)}{t^2-z^2}dt],$$
$$= 2iza^4[\frac{m^3}{k}\{\zeta_3 - \frac{z^2-b^2}{a^2-b^2}(\zeta_4 - \rho_1(z))\}$$
$$+\frac{m_2^3}{k_2}\{\tau_3 - \frac{c^2-z^2}{c^2}(\tau_4 - \rho_2(z))\}] \tag{26}$$

where

$$\zeta_i = I_i(\frac{\pi}{2},k,m) + I_i(\phi_1(a_1),k,m) - I_i(\phi_1(b_1),k,m),$$

$$\tau_i = I_i(\frac{\pi}{2},k_2,m_2) - I_i(\phi_7(c_1),k_2,m_2),$$

$$I_3(\theta,p,q) = \frac{1}{8p^2}((\frac{q}{p}-\frac{p}{q})^2 + 2p^2 + q^2(2-3p^2))\times$$
$$\Upsilon(\theta,p,q) - \frac{\sqrt{1-q^2}}{8}(\frac{1}{p^2}+\frac{1-3q^2}{q^2})E(\xi,p_1)$$
$$-\frac{1-p^2}{8\sqrt{1-q^2}}(\frac{q^2}{p^4}-\frac{3(1-q^2)}{p^2})F(\xi,p_1)$$
$$-\frac{1}{8}(3+\frac{q^2}{p^2}-q^2(3+2\sin^2\theta))N(\theta,p,q)$$

$$I_4(\theta,p,q) = \frac{1}{2}(\frac{q^2}{p^2}+1-q^2)\Upsilon(\theta,p,q)$$
$$+\frac{\sqrt{1-q^2}}{2}E(\xi,p_1) - \frac{q^2(1-p^2)}{2p^2\sqrt{1-q^2}}F(\xi,p_1)$$
$$+\frac{q^2}{2}N(\theta,p,q),$$

$$H(\theta,n,p,q) = \frac{1}{n^2}[q^2\Upsilon(\theta,p,q)$$
$$+\frac{p^2-q^2}{\sqrt{1-q^2}}F(\xi,p_1) - \frac{p^2-n^2}{\sqrt{1-q^2}}\Pi(\xi,\frac{n^2-q^2}{1-q^2},p_1)],$$

$$\Upsilon(\theta,p,q) = \frac{p}{q}\tan^{-1}(\frac{pq\cos\theta\sin\theta}{\sqrt{1-p^2\sin^2\theta}\sqrt{1-q^2\sin^2\theta}})$$
$$+\frac{1-p^2}{\sqrt{1-q^2}}\Pi(\xi,p^2,p_1),$$

$$N(\theta,p,q) = \frac{\sin\theta\cos\theta\sqrt{1-p^2\sin^2\theta}}{\sqrt{1-q^2\sin^2\theta}},$$

$$p_1 = \sqrt{\frac{p^2-q^2}{1-q^2}}, \quad \tan\xi = \sqrt{1-q^2}\tan\theta,$$

$$\rho_1(z) = H(\phi_1(a_1), n(z), k, m) - H(\phi_1(b_1), n(z), k, m) + H(\frac{\pi}{2}, n(z), k, m),$$

$$\rho_2(z) = H(\frac{\pi}{2}, n_2(z), k_2, m_2) - H(\phi_7(c_1), n_2(z), k_2, m_2),$$

$$k_2^2 = \frac{c^2}{b^2}, m^2 = \frac{a^2-b^2}{a^2}, m_2^2 = \frac{c^2}{a^2},$$

$$n^2(x) = \frac{a^2-b^2}{a^2-x^2}, n_2^2(x) = \frac{c^2}{x^2},$$

$$\sin^2\phi_1(x) = \frac{a^2-x^2}{a^2-b^2}, \sin^2\phi_7(x) = \frac{x^2}{c^2}.$$

Constants D_1, D_2 and D_3 appear in Eq.26 are evaluated using condition of single-valuedness of displacement around the rims of the cracks. However, due to symmetrical loading on the rims of yield zones, constants $D_1 = 0$ and $D_3 = 0$. Furthermore, using Eqs.12 and 25 one can evaluate

$$D_2 = -\frac{2m}{ak}(a^3 m^2\{\zeta_1 - \lambda^2\zeta_2\} + T). \tag{27}$$

where

$$I_1(\theta,p,q) = \frac{1}{24}(7 + \frac{q^2}{p^2} - q^2(3 + 2\sin^2\theta))N(\theta,p,q) + \frac{1}{24}(\frac{3}{q^2} + \frac{6-2q^2}{p^2} - \frac{q^2}{p^4} + 3q^2 - 6)\Upsilon(\theta,p,q) - \frac{E(\theta,p)}{3q^2}(1-q^2\sin^2\theta)^{3/2} - \frac{1-p^2}{24\sqrt{1-q^2}}(\frac{7-3q^2}{p^2} - \frac{q^2}{p^4})F(\xi,p_1) + \frac{\sqrt{1-q^2}}{24}(\frac{5}{q^2} + \frac{1}{p^2} - 3)E(\xi,p_1),$$

$$I_2(\theta,p,q) = \frac{q^2}{6p^2}N(\theta,p,q) + \frac{1}{6}(\frac{3-q^2}{p^2} - \frac{q^2}{p^4})\Upsilon(\theta,p,q) - \frac{1}{3q^2}(1-q^2\sin^2\theta)^{3/2}F(\theta,p) + \frac{\sqrt{1-q^2}}{6p^2}E(\xi,p_1) + \frac{1}{6\sqrt{1-q^2}}(\frac{2}{q^2} + \frac{q^2-4}{p^2} + \frac{q^2}{p^4})F(\xi,p_1)$$

$$V_2(\theta,p,q) = \frac{1}{2(p^2-1)(q^2-p^2)}[p^2E(\theta,q) + (q^2-p^2)F(\theta,q) + (2p^2q^2 + 2p^2 - p^4 - 3q^2)\Pi(\theta,p^2,q) - S(\theta,p,q)],$$

$$V_3(\theta,p,q) = \frac{1}{4(1-p^2)(q^2-p^2)}[q^2F(\theta,q) + 2p^2(1+q^2-3\frac{q^2}{p^2})\Pi(\theta,p^2,q) + 3(p^4 - 2p^2(q^2+1) + 3q^2)V_2(\theta,p,q) + \frac{S(\theta,p,q)}{1-p^2\sin^2\theta}],$$

$$T = \frac{c_1^3}{3}(E(\phi_3(c_1),k) - \lambda^2F(\phi_3(c_1),k)) + \frac{k^2T_{11}}{ba^2m^2} - \frac{1-k^2}{3b}(b^2T_{14} + T_{10}) + \frac{\lambda^2}{3b}(a^2T_9 + T_{10})],$$

$$S(\theta,p,q) = p^4\sin\theta\cos\theta\frac{\sqrt{1-q^2\sin^2\theta}}{1-p^2\sin^2\theta},$$

$$k_1^2 = k^2k_2^2, \quad \sin^2\phi_3(x) = \frac{x^2-c^2}{x^2-b^2},$$

$$\sin^2\phi_5(x) = \frac{1}{k_2^2}\sin^2\phi_3(x),$$

After a long mathematical calculation the final complex potential function $\Phi_B(z)$ for closing case may be written using Eqs.25 - 27 as

$$\Phi_B(z) = \frac{za^2\sigma_{ye}}{\pi X(z)}[\frac{m^3}{k}\{\zeta_3 - \frac{z^2-b^2}{a^2-b^2}(\zeta_4 - \rho_1(z))\} + \frac{m_2^3}{k_2}\{\tau_3 - \frac{c^2-z^2}{c^2}(\tau_4 - \rho_2(z))\} + \frac{D_2}{2a^2}] \tag{28}$$

4.2.2 Stress intensity factor

Stress intensity factors at cracks tips $t = \pm a, \pm b$ and $\pm c$ are expressed using the Eqs.16 and 28 as

$$(K_I^B)_a = \frac{2k\sigma_{ye}\sqrt{a\pi}}{m^2\pi}[\frac{m^3}{k}(\zeta_3 - \zeta_4) + \frac{m_2^3}{k_2}\{\tau_3 - (1-\frac{1}{m_2^2})(\tau_4 - \rho_2(a))\} + \frac{D_2}{2a^2}] \tag{29}$$

$$(K_I^B)_b = \frac{-2k\sigma_{ye}\sqrt{b\pi}}{m^2\pi\sqrt{1-k^2}}[\frac{m^3}{k}\zeta_3 + \frac{m_2^3}{k_2}\{\tau_3 - (1-\frac{1}{k_2^2})(\tau_4 - \rho_2(b))\} + \frac{D_2}{2a^2}] \tag{30}$$

$$(K_I^B)_c = \frac{2k^2\sigma_{ye}\sqrt{c\pi}}{m^2\pi\sqrt{1-k^2}}[\frac{m^3}{k}\{\zeta_3 - (1-\frac{1}{k^2})(\zeta_4 - \rho_1(c))\} + \frac{a^2m_2^3}{k_2}\tau_3 + \frac{D_2}{2a^2}] \tag{31}$$

4.2.3 Component of displacement

Rims of the yield zones are subjected to a quadratically varying stress distribution $\frac{t^2}{a^2}\sigma_{ye}$, therefore, component of displacement at the crack tips $\pm a_1, \pm b_1, \pm c_1$ may be written as

$$v_y^{\pm}(\pm a_1) = \mp\frac{2\sigma_{ye}}{\pi E}[A_1(\phi_1(a_1)) + A_2(\phi_1(a_1)) - \frac{D_2F(\phi_1(a_1),k)}{\sqrt{a^2-c^2}}], \tag{32}$$

International Journal of Applied Engineering Research ISSN 0973-4562 Volume 10, Number 19 (2015) pp 40010-40020

$$v_y^{\pm}(\pm b_1) = \pm\frac{2\sigma_{ye}}{\pi E}[B_1(\phi_2(b_1)) + B_2(\phi_2(b_1) + B_3(\phi_2(b_1)) - \frac{D_2 F(\phi_2(b_1),k)}{\sqrt{a^2-c^2}}], \quad (33)$$

$$v_y^{\pm}(\pm c_1) = \mp\frac{2\sigma_{ye}}{\pi E}[C_1(\phi_3(c_1)) + C_2(\phi_3(c_1)) + C_3(\phi_3(c_1)) + \frac{D_2 F(\phi_3(c_1),k)}{\sqrt{a^2-c^2}}] \quad (34)$$

(See Appendix)

5 Applications and illustrations

5.1 Growth of yield zone and load bearing capacity

Singular terms vanish at each crack tip according to Dugdale's assumption that the stresses remain finite at each crack tip. It may also be said that the stress intensity factor at each crack tip $x = \pm a, \pm b, \pm c$ must vanish i.e. $K \equiv (K_I^A)_x + (K_I^B)_x = 0$. As a result, three non-linear equations are obtained and written as

$$\frac{m^2}{k^2}(1-\lambda^2)(\frac{\sigma_\infty}{\sigma_{ye}})_a + \frac{2}{\pi}[\frac{m^3}{k}\{\zeta_3-\zeta_4\} + \frac{m_2^3}{k_2}\{\tau_3-(1-\frac{1}{n_2^2(a)})(\tau_4-\rho_2(a))\} + \frac{D_2}{2a^2}] = 0, \quad (35)$$

$$\frac{m^2}{k^2}(1-k^2-\lambda^2)(\frac{\sigma_\infty}{\sigma_{ye}})_b + \frac{2}{\pi}[\frac{m^3}{k}\zeta_3 + \frac{m_2^3}{k_2}\{\tau_3-(1-\frac{1}{n_2^2(b)})(\tau_4-\rho_2(b))\} + \frac{D_2}{2a^2}] = 0, \quad (36)$$

$$\frac{m^2}{k^2}\lambda^2(\frac{\sigma_\infty}{\sigma_{ye}})_c - \frac{2}{\pi}[\frac{m^3}{k}\{\zeta_3 - (1-\frac{1}{n^2(c)})(\zeta_4-\rho_1(c))\} + \frac{m_2^3}{k_2}\tau_3 + \frac{D_2}{2a^2}] = 0. \quad (37)$$

Yield zone length at each crack tip is then evaluated in terms of applied stress and yield stress. All the numerical results reported in this section have been obtained by using Eqs. 35,36 and 37. Behaviour of yield zone at each crack tip has been studied on increasing stresses act at the infinite boundary of the plate.

5.1.1 Three equal collinear straight cracks

A case study is presented in this section for an infinite isotropic plate under small scale yielding. Fig.4 shows the variation between normalized yield zone length, $\frac{\Gamma_6}{L_3}$, to applied load ratio, $\frac{\sigma_\infty}{\sigma_{ye}}$, at crack tip a_1. Value of $\rho = \frac{2c_1}{b_1+c_1}$ denotes the ratio between half crack length of middle crack and the distance of mid point of two neighbouring cracks from the origin. It has been observed from the Fig.4 that the length of yield zone increases as stresses applied at the boundary of the plate increased. For a value of normalized yield zone length (say 0.2), plate can bear more load when the cracks are situated far away from each other (say $\rho = 0.1$) and comparatively less load when cracks are situated close to each other (say $\rho = 0.9$).

The numerical results are compared with the results of two equal cracks having same position on real axis as two outer cracks in Fig.1 and same mechanical loading conditions.

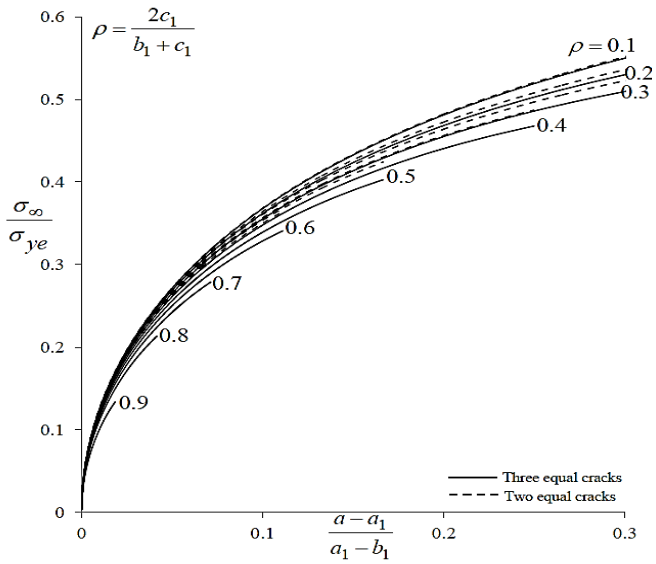

Figure 4: Normalized yield zone length $\frac{\Gamma_6}{L_3}$ to applied stress $(\frac{\sigma_\infty}{\sigma_{ye}})_a$.

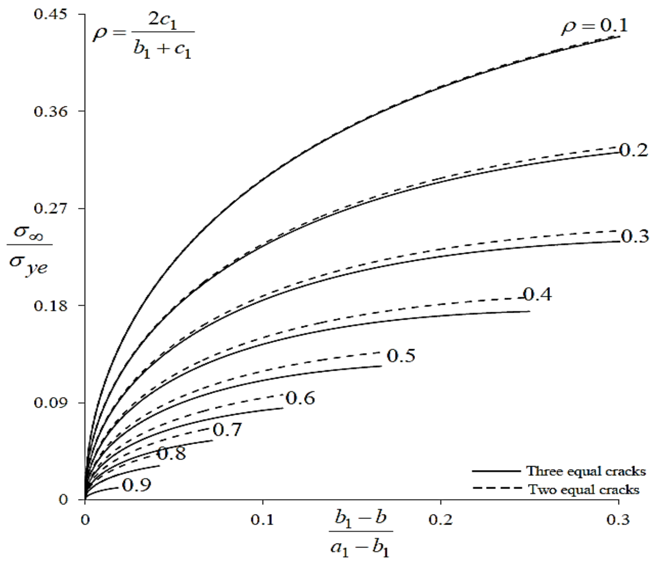

Figure 5: Normalized yield zone length $\frac{\Gamma_5}{L_3}$ to applied stress $(\frac{\sigma_\infty}{\sigma_{ye}})_b$.

It may be noted that the load ratio at the outer crack tip $t = a_1$, when three cracks are situated far away from each other, is same as the load ratio at outer crack tip of two equal cracks. This means outer cracks are very less affected by internal crack when $\rho = 0.1$ and highly affected when $\rho = 0.9$.

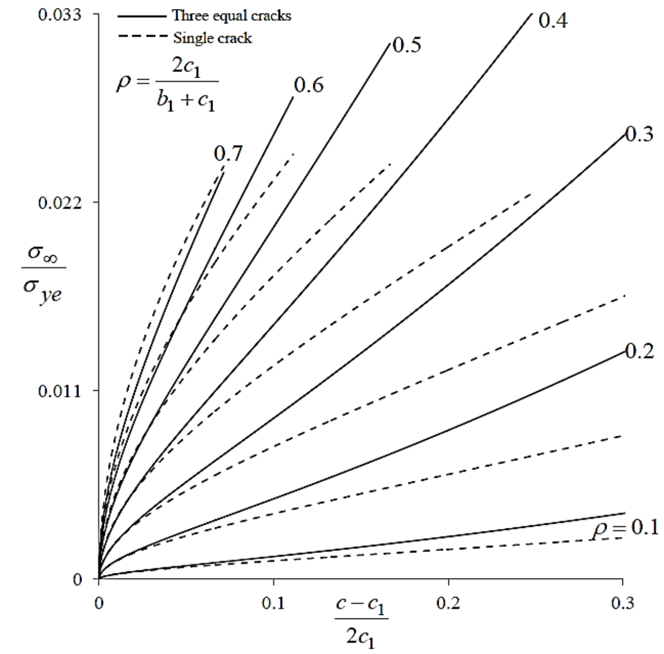

Figure 6: Normalized yield zone length $\frac{\Gamma_4}{L_2}$ to applied stress $(\frac{\sigma_\infty}{\sigma_{ye}})_c$.

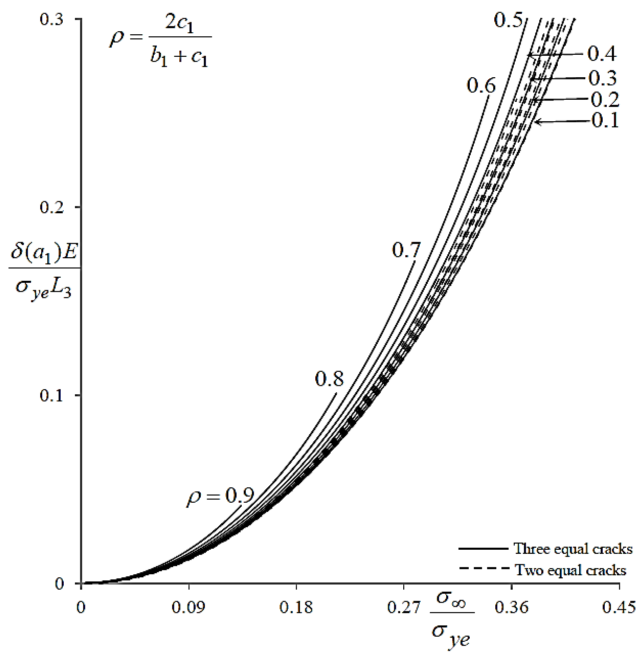

Figure 7: $(\frac{\sigma_\infty}{\sigma_{ye}})_a$ to $\frac{\delta(a_1)E}{L_3\sigma_{ye}}$

Same variation is plotted at the crack tip $t = b_1$ in Fig.5. As far as behaviour of load ratio and yield zone length is concern it is same but yield zone length Γ_5 is bigger than the yield zone length Γ_6 as expected. Furthermore, when $\rho = 0.1$ yield zone length at crack tip $t = b_1$ for three equal cracks and two equal cracks are same but a significant difference in yield zone length is seen when $\rho = 0.9$. It happens because when cracks situated closer to each other there is no crack between two equal cracks but there is an internal crack in case of three equal cracks.

Fig.6 shows the variation between normalized yield zone length and applied load ratio at the crack tip $t = c_1$. It may be noted that the quadratically varying stress distribution, $\frac{t^2}{a^2}\sigma_{ye}$, (applied on the rims of the yield zone) is very low at $\rho = 0.1$ due to large value of a^2. As a results length of yield zone, $|c - c_1|$, is very large. But when cracks are assume to be located close to each other than due small value of a^2 quadratically varying stress distribution is comparatively high, hence length of yield zone, $|c - c_1|$, is less in comparison to the case of $\rho = 0.1$.

The results so obtained are compared with the results of a single crack of length $2c_1$ under same mechanical loading conditions. Length of yield zone Γ_4 is comparatively less in case of three equal cracks when $\rho = 0.7$ and bigger when $\rho = 0.1$. This is because outer cracks suppress middle crack when situated very close. Hence, yield zone length at the tips of middle crack is small due to the presence of outer cracks. It may be noted that the effect of outer cracks on the inner crack can be measure when all cracks are situated close to each other.

5.2 Crack-tip opening displacement

Using complex variable method, analytical expressions are obtained for crack tip opening displacement $\delta(x)$ at each crack tip, $x = \pm a_1, \pm b_1, \pm c_1$ using formulae given in [6], [11],

$$\delta(x) = [v_\infty^+(x) + v_{ye}^+(x)) - (v_\infty^-(x) + v_{ye}^-(x)]. \tag{38}$$

Thus the analytical expressions for CTOD at each inner crack tip $\pm a_1$, $\pm b_1$ and $\pm c_1$ be evaluated by putting the corresponding values of $v_\infty^\pm(x)$ and $v_{ye}^\pm(x)$ from Eqs.20 - 22 and 32 - 34 into Eq. 38, one may found three non-linear equations for crack tip opening displacement(CTOD) as:

$$\delta(a_1) = \frac{4\sigma_{ye}}{E}[\frac{am}{k}(E(\phi_1(a_1),k) - \lambda^2 F(\phi_1(a_1),k)) \times$$
$$(\frac{\sigma_\infty}{\sigma_{ye}})_a - \frac{1}{\pi}(A_1(\phi_1(a_1)) + A_2(\phi_1(a_1)) \tag{39}$$
$$-\frac{kD_2}{am}F(\phi_1(a_1),k))],$$

$$\delta(b_1)=\frac{4\sigma_{ye}}{E}[\frac{am}{k}(E(\phi_2(b_1),k)-\frac{k^2 \sin\phi_2(b_1)\cos\phi_2(b_1)}{\sqrt{1-k^2\sin^2\phi_2(b_1)}}$$
$$-\lambda^2F(\phi_2(b_1),k))(\frac{\sigma_\infty}{\sigma_{ye}})_b-\frac{1}{\pi}(B_1(\phi_2(b_1))+B_2(\phi_2(b_1)) \quad (40)$$
$$+B_3(\phi_2(b_1))-\frac{kD_2}{am}F(\phi_2(b_1),k))],$$

$$\delta(c_1)=\frac{4\sigma_{ye}}{E}[\frac{am}{k}(-E(\phi_3(c_1),k)+$$
$$\tan\phi_3(c_1)\sqrt{1-k^2\sin^2\phi_3(c_1)}+\lambda^2F(\phi_3(c_1),k))(\frac{\sigma_\infty}{\sigma_{ye}})_c \quad (41)$$
$$-\frac{1}{\pi}(C_1(\phi_3(c_1))+C_2(\phi_3(c_1))+C_3(\phi_3(c_1))$$
$$+\frac{kD_2}{am}F(\phi_3(c_1),k))].$$

5.2.1 Three equal collinear straight cracks

Consider three equal cracks weaken an isotropic infinite plate as shown in fig.1. This section deals with the normalized CTOD, $\frac{\delta(x)E}{L_i\sigma_{ye}}$, at each crack tip due to remotely applied stresses at the boundary of the plate. Fig.7 shows the variation between applied load ratio $\frac{\sigma_\infty}{\sigma_{ye}}$ and normalized CTOD $\frac{\delta(a_1)E}{L_3\sigma_{ye}}$ at the crack tip a_1.

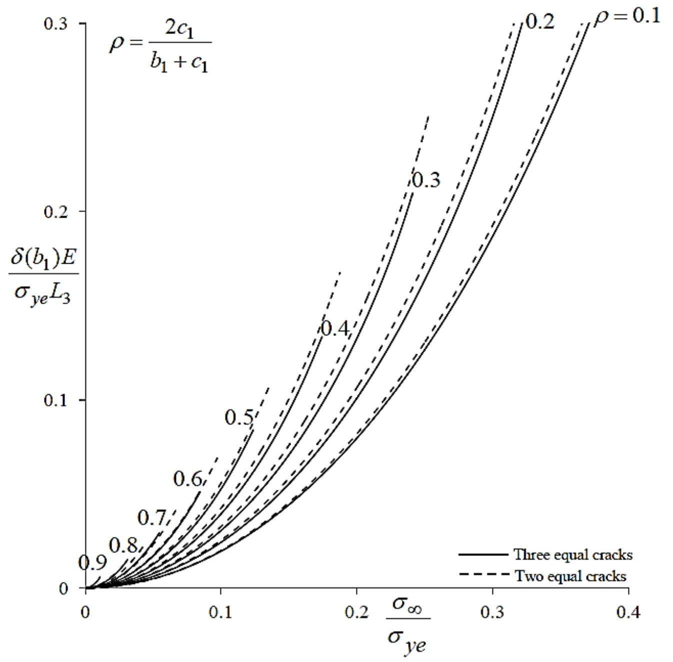

Figure 8: $(\frac{\sigma_\infty}{\sigma_{ye}})_b$ **to** $\frac{\delta(b_1)E}{L_3\sigma_{ye}}$

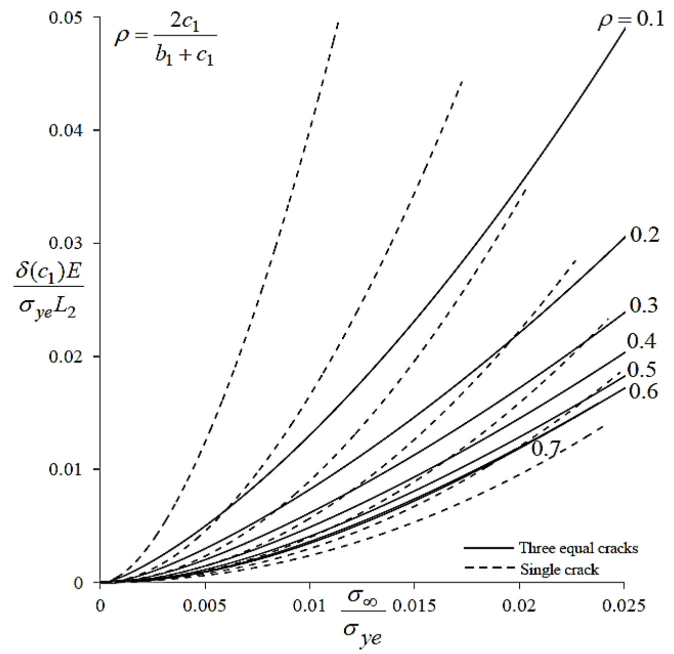

Figure 9: $(\frac{\sigma_\infty}{\sigma_{ye}})_c$ **to** $\frac{\delta(c_1)E}{L_2\sigma_{ye}}$

It has been observed that opening of cracks increases as stresses applied at the boundary of the plate increase. Opening of cracks at tip a_1 is larger when outer cracks are situated close to the middle crack ($\rho=0.9$) in comparison to situation when outer cracks are placed far away from middle crack ($\rho=0.1$).

Same variation has been plotted for crack tip b_1, shown in fig.8, when $\rho=0.1$ insignificant difference is seen between the results of three equal cracks and two equal cracks, means opening of cracks at tip b_1 is almost same in case of outer cracks placed away from the middle cracks but when $\rho=0.9$ the difference between the opening of cracks is significantly different.

Opening of central crack is compared with the opening of an equivalent single crack of length $2c_1$ (fig.9) under same mechanical loading conditions using relation given in [4]. Opening of central crack is larger in case of $\rho=0.1$ in comparison to the case when $\rho=0.7$ under the influence of outer cracks. When $\rho=0.1$ single crack opens more than the central crack of three equal cracks due to the existence of two neighbouring cracks. Furthermore, almost same opening is shown by central crack and equivalent single crack when $\rho=0.7$ because entire configuration of three cracks behave like as a single crack (since they are close to each other).

6.Validation of mathematical expressions

Mathematical expressions given in Eq.35 for remotely applied stress and in Eq.39 for CTOD at the crack tip $t=a_1$ after

International Journal of Applied Engineering Research ISSN 0973-4562 Volume 10, Number 19 (2015) pp 40010-40020

putting $b = b_1$, $c = c_1$ and $b = c = 0$ agreed with the results obtained by Harrop[4] for a single crack of length $2a_1$ when yield zones are subjected to quadratically varying stress distribution.

7.Conclusion

Dugdale model has been modified for three equal collinear straight cracks for quadratically varying stress distribution. Closed form solution is obtained for stress intensity factor and crack tip-opening displacement using complex variable method. Load bearing capacity of an infinite plate is examined in the presence of three equal collinear straight cracks with respect to yield zone length. Numerical results are obtained for applied load ratio, yield zone length and crack tip-opening displacement. The results are compared with the results of two equal symmetrically situated cracks when yield zone are subjected to parabolic yield stress distribution.

Acknowledgement

First author is thankful to University Grant Commission, Govt. of India for providing BSR fellowship.

Appendix

The quantities used in the above expressions are

$$A_1(\theta) = \frac{2ik}{3a^3m}[\frac{a_1^3 X(a_1)}{a^2 - a_1^2}(F(\theta,k) - \Pi(\theta, \frac{k^2}{\alpha_1^2(a_1)}, k))$$
$$-\frac{b_1^3 X(b_1)}{a^2 - b_1^2}\Pi(\theta, \alpha_1^2(b_1), k) + \frac{c_1^3 X(c_1)}{a^2 - c_1^2}\Pi(\theta, \alpha_1^2(c_1), k)],$$

$$A_2(\theta) = \frac{2}{3a^2b}[E(\theta,k)\{\hbar_2 + c^2(T_1 + T_5) - a^2 T_9\} -$$
$$\frac{k^2 F(\theta,k)}{a^2m^2}\{\hbar_3 + b^2 T_2 + a^2(T_6 + T_{13})\}$$
$$+ a^2m^2 N(\theta,k,0)(\hbar_1 + a_1^4 \hbar_4)$$
$$-\frac{a_1^3 b}{2} log\,|\frac{X^2(a_1)}{a_1^2[(a^2 - a_1^2)^2 - k^2(a^2 - c^2)^2]} - 1|],$$

$$B_1(\theta) = \frac{2b}{3}G_1(\theta)[T_{15} - T_{16}(\frac{m_2^2 F(\theta,k)}{G_1(\theta)} + \frac{m^2}{k^2})]$$
$$-2am^2 F(\theta,k)(\zeta_3 + (1 - \frac{1}{k^2})\zeta_4 + \frac{bkm_2^2}{am^3}\tau_3)$$
$$+\frac{2am^2}{k^2}G_1(\theta)(\zeta_4 - \frac{bk}{am}\tau_4) - \mu_1(2(k^2 - 1)F(\theta,k)$$
$$+(2 - k^2)G_1(\theta) + N(\theta,0,k)(\frac{k^2(1-k^2)}{1 - k^2\,sin^2\theta}))$$

$$B_2(\theta) = \frac{2ik}{3a^3m}[\vartheta(b_1,4,2) + T_{17}G_1(\theta) + (\frac{X(a_1)}{a_1(c^2 - a_1^2)}$$
$$-\frac{X(b_1)}{b_1(c^2 - b_1^2)} + \frac{X(c_1)}{c_1\alpha_6^2(c_1)(c^2 - c_1^2)})c^4 F(\theta,k)$$
$$+(b^2 - c^2)(\frac{a_1^3(a^2 - a_1^2)}{X(a_1)}\Pi(\theta, \alpha_2^2(a_1), k) -$$
$$\frac{b_1^3(a^2 - b_1^2)}{X(b_1)}(F(\theta,k) - \Pi(\theta, \alpha_3^2(b_1), k))$$
$$+\frac{c_1^3(a^2 - c_1^2)}{X(c_1)}\Pi(\theta, \alpha_2^2(c_1), k))],$$

$$B_3(\theta) = \frac{2a^2m^2}{3bk^2}F(k_1)[(1 - k^2)F(\theta,k) - (1 + k^2)G_1(\theta)$$
$$+\frac{k^2(1-k^2)}{1 - k^2\,sin^2\theta}N(\theta,0,k) + \frac{F(\phi_6(c_1),k_1)}{F(k_1)}(G_1(\theta)$$
$$-(1 - k^2)F(\theta,k) - \frac{G_2(\theta)}{1 - m_2^2})] + \mu_2[(1 - k^2)F(\theta,k) -$$
$$(1 + \frac{a^2 + 2b^2}{a^2 - c^2})G_1(\theta) + \frac{(k^2 - k^4)N(\theta,0,k)}{1 - k^2\,sin^2\theta}]$$
$$-\frac{b_1^3}{3a^2}log\,|\frac{X^2(b_1)}{b_1^2[(a^2 - b_1^2)^2 - \frac{a^4m^4}{k^2}]} - 1|,$$

$$C_1(\theta) = 2am^2 F(\theta,k)(\zeta_3 + (1 - \frac{1}{k^2})\zeta_4 + \frac{bkm_2^2}{am^3}\tau_3)$$
$$+\frac{2b}{3}G_2(\theta)[T_{15} + T_{16}(\frac{m_2^2 F(\theta,k)}{G_2(\theta)} - \frac{m^2}{k^2})]$$
$$+\frac{2am^2}{k^2}G_2(\theta)(\zeta_4 - \frac{bk}{am}\tau_4) - \mu_1[2(1 - k^2)F(\theta,k)$$
$$+(2 - k^2)G_2(\theta) + N(\theta,k,0)(\frac{1-k^2}{cos^4\theta})],$$

$$C_2(\theta) = -\frac{2ik}{3a^3m}[\vartheta(c_1,6,1)$$
$$+(\frac{b^2c^2 + a_1^2(b^2 - c^2)}{a_1(b^2 - a_1^2)}X(a_1)$$
$$-\frac{b^2c^2 + b_1^2(b^2 - c^2)}{b_1(b^2 - b_1^2)}X(b_1)$$
$$+\frac{c^4 X(c_1)}{c_1\alpha_6^2(c_1)(c^2 - c_1^2)})F(\theta,k)$$
$$-(b^2 - c^2)(\frac{a_1^3(a^2 - a_1^2)}{X(a_1)}\Pi(\theta, \alpha_3^2(a_1), k)$$
$$-\frac{b_1^3(a^2 - b_1^2)}{X(b_1)}\Pi(\theta, \alpha_3^2(b_1), k)$$
$$-\frac{c_1^3(a^2 - c_1^2)}{X(c_1)}\Pi(\theta, \alpha_2^2(c_1), k)) - T_{17}G_2(\theta)],$$

$$C_3(\theta) = -\frac{2a^2m^2}{3bk^2}F(k_1)[(1-k^2)F(\theta,k)$$
$$+(1+k^2)G_2(\theta) - N(\theta,k,0)\frac{1-k^2}{cos^4(\theta)}$$
$$-\frac{F(\phi_6(c_1),k_1)}{F(k_1)}(G_2(\theta)+(1-k^2)F(\theta,k)-\frac{G_1(\theta)}{1-m_2^2})]$$
$$-\mu_2[(1+\frac{a^2+2b^2}{a^2-c^2})G_2(\theta)+(1-k^2)F(\theta,k)$$
$$-\frac{1-k^2}{cos^4\theta}N(\theta,k,0)] - \frac{c_1^3}{3a^2}log\,|\frac{X^2(c_1)}{c_1^2[(a^2-c_1^2)^2-\frac{a^4m^4}{k^2}]}+1|,$$
$$\hbar_i = T_i + T_{i+4} - T_{i+8} + \frac{(i-1)(i-2)(i-3)}{6a_1^2}\times$$
$$[F(\phi_4(a_1),k_1)+F(\phi_2(b_1),k_1)-F(\phi_5(c_1),k_1)],$$
$$k_3^2 = \frac{b^2-a^2}{b^2}, \alpha_1^2(x) = \frac{(a^2-b^2)}{(a^2-x^2)},$$
$$\alpha_3^2(x) = \frac{(x^2-b^2)}{(x^2-c^2)}, \alpha_2^2(x) = \frac{k^2}{\alpha_3^2(x)},$$
$$\alpha_4^2(x) = \frac{x^2}{b^2}\alpha_1^2(x), \alpha_5^2(x) = k_2^2\alpha_3^2(x),$$
$$\alpha_6^2(x) = \frac{k_1^2}{\alpha_4^2(x)}, sin^2\phi_i(x) = \frac{1}{\alpha_i^2(x)},$$
$$G_1(\theta) = E(\theta,k) - \frac{k^2\,sin\theta\,cos\theta}{\sqrt{1-k^2\,sin^2\theta}},$$
$$G_2(\theta) = tan\theta\sqrt{1-k^2\,sin^2\theta} - E(\theta,k),$$
$$\vartheta(r,i,j) = \frac{a^2r^2X(r)}{b(a^2-r^2)}(\Pi(\phi_4(a_1),\alpha_4^2(r),k_1)$$
$$-F(\phi_i(r),k_1)+(-1)^j\,\Pi(\phi_4(b_1),\alpha^2_{i+2(-1)^j}(r),k_1)$$
$$+(-1)^{j+1}\Pi(\phi_6(c_1),\alpha^2_{i+2(-1)^j}(r),k_1)),$$
$$\mu_1 = \frac{2am^4}{3k^4}\{\Upsilon(\phi_1(a_1),k,m)-\Upsilon(\phi_1(b_1),k,m)$$
$$+\Upsilon(\frac{\pi}{2},k,m)+\frac{ak^2m_2^2}{bm^2}(F(k_1)+F(\phi_4(a_1),k_1)$$
$$-F(\phi_4(b_1),k_1))\},$$
$$\mu_2 = \frac{2bm^3}{3k^3}\{\Upsilon(\phi_7(c_1),k_2,m_2)-\Upsilon(\frac{\pi}{2},k_2,m_2)$$
$$-\frac{a^2mk}{b^2}F(k_1)(1-\frac{F(\phi_6(c_1),k_1)}{F(k_1)})\},$$
$$T_1 = a^2\Pi(\phi_4(a_1),k_3^2,k_1),$$
$$T_2 = \frac{a^2b^2m^2}{2k^2}[E(\phi_4(a_1),k_1)+(\frac{k_1^2}{k_3^2}-1)F(\phi_4(a_1),k_1)$$
$$+(2-k_3^2-\frac{k_1^2}{k_3^2})\Pi(\phi_4(a_1),k_3^2,k_1)-\frac{S(\phi_4(a_1),k_3,k_1)}{k_3^2}],$$
$$T_3 = -\frac{a^4b^2m^2}{k^2}[\frac{k_1^2}{k_3^2}\Pi(\phi_4(a_1),k_3^2,k_1)$$
$$+(k_1^2-\frac{2k_1^2}{k_3^2}+1)V_2(\phi_4(a_1),k_3,k_1)$$
$$+(k_3^2-1)(1-\frac{k_1^2}{k_3^2})V_3(\phi_4(a_1),k_3,k_1)],$$
$$T_4 = \frac{\alpha_1^2(a_1)}{a^2m^2}[F(\phi_4(a_1),k_1)$$
$$-(1-\frac{k_3^2}{\alpha_4^2(a_1)})\Pi(\phi_4(a_1),\alpha_6^2(a_1),k_1)],$$
$$T_5 = b^2[k_2^2F(\phi_2(b_1),k_1)+(1-k_2^2)\Pi(\phi_2(b_1),k^2,k_1)],$$
$$T_6 = \frac{a^2b^2m^2}{2k^2}[E(\phi_2(b_1),k_1)+(k_2^2-1)F(\phi_2(b_1),k_1)$$
$$+(2-k^2-k_2^2)\Pi(\phi_2(b_1),k^2,k_1)-\frac{S(\phi_2(b_1),k,k_1)}{k^2}],$$
$$T_7 = \frac{a^2b^4m^2(k_2^2-1)}{k^2}[k_2^2\Pi(\phi_2(b_1),k^2,k_1)$$
$$+(k_1^2-2k_2^2+1)V_2(\phi_2(b_1),k,k_1)$$
$$+(k^2-1)(1-k_2^2)V_3(\phi_2(b_1),k,k_1)],$$
$$T_8 = \frac{1}{b^2-a_1^2}[(1-\alpha_3^2(a_1))\Pi(\phi_2(b_1),\alpha_2^2(a_1),k_1)$$
$$+\alpha_3^2(a_1)F(\phi_2(b_1),k_1)],$$
$$T_9 = b^2[F(\phi_5(c_1),k_1)+(k_2^2-1)\Pi(\phi_5(c_1),k_2^2,k_1)],$$
$$T_{10} = \frac{a^2b^2m^2}{2k^2}[E(\phi_5(c_1),k_1)-(1+k^2)F(\phi_5(c_1),k_1)$$
$$-(k_2^2-k^2)\Pi(\phi_5(c_1),k_2^2,k_1)-\frac{S(\phi_5(c_1),k_2,k_1)}{k_2^2}],$$
$$T_{11} = \frac{a^2b^4m^2(1-k_2^2)}{k^2}[-k^2F(\phi_5(c_1),k_1)$$
$$+(3k^2-k_1^2-1)\Pi(\phi_5(c_1),k_2^2,k_1)$$
$$+(2k_1^2-3k^2-k_2^2+2)V_2(\phi_5(c_1),k_2,k_1)$$
$$+(k_2^2-1)(1-k^2)V_3(\phi_5(c_1),k_2,k_1)],$$
$$T_{12} = \frac{1}{b^2-a_1^2}[F(\phi_5(c_1),k_1)$$
$$+(\alpha_3^2(a_1)-1)\Pi(\phi_5(c_1),\alpha_5^2(a_1),k_1)],$$
$$T_{13} = \frac{b^4k_3^2}{2k^2}[E(\phi_5(c_1),k_1)+(1-k^2)F(\phi_5(c_1),k_1)$$
$$+(k_2^2+k^2-2)\Pi(\phi_5(c_1),k_2^2,k_1)$$
$$-\frac{S(\phi_5(c_1),k_2,k_1)}{k_2^2}],$$
$$T_{14} = \frac{b^2}{1-k^2}[E(\phi_5(c_1),k_1)+(k_2^2-1)k^2F(\phi_5(c_1),k_1)$$
$$+(k_2^2-1)(1-k^2)\Pi(\phi_5(c_1),k_2^2,k_1)]$$

$$T_{15} = F(\phi_4(a_1), k_1) - F(\phi_4(b_1), k_1),$$
$$T_{16} = E(\phi_4(a_1), k_1) - E(\phi_4(b_1), k_1) + E(\phi_6(c_1), k_1),$$
$$T_{17} = (a^2 - c^2)(\frac{X(a_1)}{a_1} - \frac{X(b_1)}{b_1} - \frac{c_1 X(c_1)}{a^2 - c_1^2}).$$

References

[1] B. David, , "Elementary Engineering Fracture Mechanics", Martinus Nijhoff Publishers, The Netherlands, 1982.

[2] D. S. Dugdale, "Yielding of steel sheets containing slits," Journal of the Mechanics and Physics of Solids, Vol. 8, pp. 100-104,1960.

[3] M. F. Kanninen, "A solution for a Dugdale crack subjected to a linearly varying tensile loading," International Journal of Engineering Science, Vol. 8, pp. 85-95, 1970.

[4] L. P. Harrop, "Application of a modified Dugdale model to the K vs COD relation," Engineering Fracture Mechanics, Vol. 10, pp. 807-816, 1978.

[5] P. S. Theocaris and E. E. Gdoutos, "The modified Dugdale-Barenbaltt model adapted to various configurations in metals," International Journal of Fracture, Vol. 10, no 4, pp. 549-564, 1974.

[6] G. C. Sih and X. S. Tang, "Dual scaling damage model associated with weak singularity for macroscopic crack possessing a micro/mesoscopic notch tip," Theoretical and Applied Fracture Mechanics, Vol. 42 no 1, pp. 1-24, 2004.

[7] X. S. Tang and C. H. Gao, "Macro–micro dual scale crack model linked by a restraining stress zone with a linear distribution," Theoretical and Applied Fracture Mechanics, Vol. 71, pp. 31-43, 2014.

[8] P. S.Theocaris, "Dugdale models for two collinear unequal cracks," Engineering Fracture Mechanics, Vol. 18 no 3, pp. 549-559, 1983.

[9] R. A. Collins and D. J. Cartwright, "An analytical solution for two equal-length collinear strips yield cracks," Engineering Fracture Mechanics, Vol. 68, pp. 915-924, 2001.

[10] S. Hasan and N.Akthar, "Dugdale model for three equal collinear straight cracks: An analytical approach" ,Theoretical and Applied Fracture Mechanics, Vol. 78, pp. 40-50,2015.

[11] X.Q. Feng and D. Gross, "On the coalescence of collinear cracks in quasi-brittle materials," Engineering Fracture Mechanics, Vol. 65, pp. 511-524, 2000.

[12] R. R.Bhargava, andS. Hasan, "The Dugdale solution for two unequal straight cracks weakening in an infinite plate," Sadhana-Academy Proceeding in Engineering Sciences, Vol. 35, no 1, pp. 19-29, 2010.

[13] R. R. Bhargava, and S. Hasan, "Crack opening displacement for two unequal straight cracks with coalesced plastic zones–A modified Dugdale model", Applied Mathematical Modelling, Vol. 35, no 8, pp. 3788-3796, 2011.

[14] R. R. Bhargava and S. Hasan, "Crack-tip-opening displacement for four symmetrically situated cracks with coalesced interior yield zones," Applied Mathematical Modelling, Vol. 36, no 11, pp. 741-5749, 2012.

[15] R. R. Bhargava and S. Hasan, "Mathematical model for crack arrest of an infinite plate weakened by a finite and two semi-infinite cracks", Applied Mathematics and Computation, Vol. 218 , no 11, pp. 6576-6584, 2012.

[16] W. Xu and X. R. Wu, "Weight functions and strip-yield model analysis for three collinear cracks," Engineering Fracture Mechanics, Vol. 85, pp. 73-87, 2012.

[17] E. E. Gdoutos, "Fracture Mechanics - An Introduction", Second Edition, Springer, The Netherlands, 2005.

[18] N. I. Muskhelishvili, "Some Basic Problems of Mathematical Theory of Elasticity", Leiden: P. Noordhoff, 1963.

[19] P. F. Byrd and M. D.Friedman, "Handbook of Elliptical Integrals for Engineers and Scientist", Springer-Verlag New York Heidelberg Berlin, 1971.

[20] H. Tada, P. C. Paris and G. R. Erwin, "The Stress Analysis of Cracks Handbook", 3rd ed. ASME Press New York, 2000.